HEAT AND MASS TRANSFER PERFORMANCE AND EXERGY PERFORMANCE EVALUATION OF SEAWATER COOLING TOWER CONSIDERING DIFFERENT INLET PARAMETERS

by

Yang YU[a], Xiaoni QI[a*], Xiaochen HOU[a], Xiaohang QU[a], Qianjian GUO[b], and Hegang ZHU[a]

[a] College of Traffic and Vehicle Engineering, Shandong University of Technology, Zibo, China
[b] College of Mechanical Engineering, Shandong University of Technology, Zibo, China

Original scientific paper
https://doi.org/10.2298/TSCI210523312Y

Cooling towers are important components within re-circulating cooling water systems. Due to a shortage of freshwater resources, seawater cooling towers are widely used both in manufacturing and everyday life. This paper researches the mechanical draft counterflow wet seawater cooling tower, and establishes and verifies a detailed thermal performance calculation model. Referring to the Second law of thermodynamics, the heat and mass transfer performance and exergy performance of the seawater cooling tower were studied. The effects of salinity, inlet air speed, and air wet-bulb temperature on the cooling efficiency, thermal efficiency, and exergy efficiency were analyzed. The results show that compared to the air wet-bulb temperature, changes in air speed have more influence on cooling and thermal efficiency under the study conditions. Moreover, the air wet-bulb temperature is the significant parameter affecting exergy efficiency. With an increase in salinity, the cooling, thermal, and exergy efficiency are about 2.40-8.25%, 1.06-3.09%, and 2.47-7.73% lower than that of freshwater, respectively, within an air speed of 3.1-3.6 m/s. With an increase in salinity, the cooling, thermal, and exergy efficiency are about 2.28-8.47%, 1.03-3.37%, and 2.44-7.99% lower than that of freshwater, respectively, within an air wet-bulb temperature of 25-27 °C. Through the exergy analysis of the seawater cooling tower, it is obvious that the heat and mass transfer performance and exergy performance can be improved by selecting the optimum operating conditions and appropriate packing specifications.

Key words: *seawater cooling tower, heat and mass transfer, exergy analysis, performance evaluation, modelling*

Introduction

The shortage of freshwater resources is becoming increasingly serious, but the demand for cooling water is increasing for production and everyday living purposes (such as petrochemical and thermal power plants, and central air-conditioning systems). Therefore, seawater circulation cooling technology is currently attracting increased attention. In coastal areas, using seawater instead of freshwater as circulating cooling water (including in seawater cooling tower applications) cannot only relieve the pressure of marine thermal pollution but could also be valuable in solving the freshwater shortage problem [1-4].

* Corresponding author, e-mail: bmjw@163.com

Currently, thermal performance studies of cooling towers generally focus on freshwater towers and are primarily based on the First law of thermodynamics (energy analysis) [5-10], with only a few studies existing on the Second law of thermodynamics (exergy analysis), which are also based on freshwater towers. Muangnoi [11] and Muangnoi *et al.* [12] studied the changes of water exergy, air exergy, and exergy destruction with different height cooling towers. Qureshi and Zubair [13] analyzed the impact of inlet parameters on cooling tower exergy performance, but all the inlet water chemical exergy (including the chemical exergy of unevaporated water) was used as part of the input to evaluate the performance, resulting in the exergy efficiency being close to 100%, therefore, overestimating the cooling tower exergy performance. Consequently, there is comparatively little research, using the exergy analysis method, to evaluate seawater cooling tower thermal performance. Sharqawy *et al.* [14, 15] studied the effect of salinity on air and water effectiveness by developing a numerical model for seawater cooling towers. They formulated a correction factor equation representing the effectiveness of seawater and freshwater cooling towers under the same operating conditions and tower specifications. Qi *et al.* [16] studied a seawater shower cooling tower, without packing, and established a complete mathematical model suitable for performance analysis. By establishing a 3-D numerical model, Sadafi *et al.* [17] simulated the performance difference between seawater and freshwater in a spray cooling system, Wan *et al.* [18] studied the cooling performance of a natural draft wet cooling tower, and also analyzed the effects of salinity and ambient crosswind on outlet water temperature, ventilation rate, and circulating water evaporation.

In this study, a detailed thermodynamic performance calculation model of the mechanical draft counterflow wet seawater cooling tower (MDCWSCT) based on the Poppe model [19] was established to solve the outlet parameters of seawater and air numerically, which was validated by comparison with the experimental results obtained from literature. The heat and mass transfer performance and exergy performance of the seawater tower were evaluated by using the performance evaluation index (cooling efficiency, thermal efficiency, and exergy efficiency). The influences of salinity, inlet air speed, and inlet air wet-bulb temperature on the performance evaluation index were analyzed, providing a reference for the actual operation of seawater cooling towers.

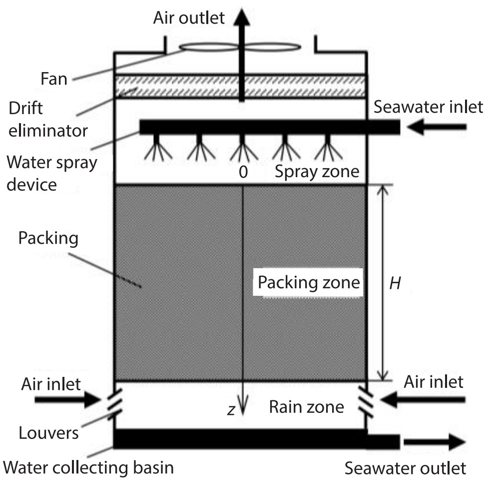

Figure 1. Schematic diagram of the MDCWSCT

Physical model

Cooling towers are used to dissipate waste heat from hot circulating cooling water into the environment. The schematic diagram of the MDCWSCT is shown in fig. 1. Seawater is the given circulating cooling water, carrying waste heat, falling from the top to the bottom of the tower. Ambient air enters at the bottom and escapes from the top of the tower through the packing zone. The water temperature is gradually decreased along with evaporation and increasing air temperature and humidity. The gas-liquid two-phase heating and mass transfer process occurs in the packing zone. During actual operation a significant part (more than 80%) of the total heat and mass transfer in cooling towers occurs in the packing zone [20]. Consequently the packing zone is the main research object of this paper. A mathematical co-ordinate system was established for the packing zone, taking the vertical downward as the positive direction. The co-ordinate origin is located at the inlet of the packing zone ($z = 0$), and the outlet of the packing zone is $z = H$.

Mathematical model

To establish the heat and mass transfer governing equations and the exergy analysis equations, a control volume was considered as shown in fig. 2. The impact of water mass-flow loss, due to evaporation, on the air physical parameters, along with the tower and the Lewis factor variation, $\mathrm{Le_f}$, are all accounted for in the mathematical model. The main assumptions of the model are given below [10, 14]:

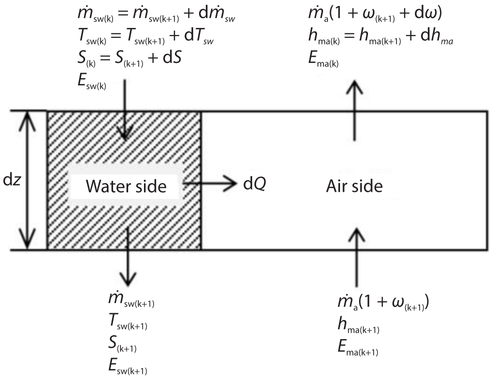

Figure 2. Control volume of the packing zone

- The physical values at any cross-section of the tower are uniform, which only changes along the z-axis.
- The air and water contact process in the packing zone can be regarded as a steady-state process so that the mathematical model is a 1-D steady-state model.
- The heat and mass transfer between air and water occurs in the direction perpendicular to the tower wall, the resistance of heat transfer in the water film is negligible (*i.e.* the internal and external temperature of the water film is consistent during heat and mass transfer).
- Droplets of seawater drifting into the environment through a drift eliminator are ignored.
- There is no energy or mass exchange to the environment, and only negligible heat and mass transfer from the fan to air or water streams.
- The atmospheric pressure in the tower remains constant (101325 Pa).

The governing equations of heat and mass transfer

According to the control volume in fig. 2, the mass and energy balance of the seawater-side and air-side on the differential height, dz, can be written as eqs. (1)-(3), which describes the change rate of seawater mass-flow rate, $\dot{m}_{\mathrm{sw}}$, air humidity ratiom, ω, and seawater temperature, T_{sw}, along the z-axis [6, 20]:

$$\frac{\mathrm{d}m_{\mathrm{sw}}}{\mathrm{d}z} = K_{\mathrm{D}} A \left(\omega_{\mathrm{s,w}} - \omega\right) \tag{1}$$

$$\frac{\mathrm{d}\omega}{\mathrm{d}z} = \frac{K_D A}{\dot{m}_{\mathrm{a}}}\left(\omega_{\mathrm{s,w}} - \omega\right) \tag{2}$$

$$\frac{\mathrm{d}T_{\mathrm{sw}}}{\mathrm{d}z} = \frac{\dot{m}_{\mathrm{a}}}{\dot{m}_{\mathrm{sw}}}\left[\frac{1}{c_{p,\mathrm{sw}}}\frac{\mathrm{d}h_{\mathrm{ma}}}{\mathrm{d}z} - \left(T_{\mathrm{sw}} - 273.15\right)\frac{\mathrm{d}\omega}{\mathrm{d}z}\right] \tag{3}$$

where K_{D}, A, $\omega_{\mathrm{s,w}}$, $\dot{m}_{\mathrm{a}}$, and $c_{p,\mathrm{sw}}$ are the volumetric mass transfer coefficient, packing cross-section area, saturated moist air humidity ratio at water temperature, air mass-flow rate, and seawater specific heat, respectively.

The energy balance at the interface between the water-side and the air-side can be expressed as eq. (4), which describes the change rate of air specific enthalpy, h_{ma}, along the z-axis [6, 20]:

$$\frac{\mathrm{d}h_{\mathrm{ma}}}{\mathrm{d}z}=\frac{K_{\mathrm{D}}A}{\dot{m}_{\mathrm{a}}}\left[\mathrm{Le_f}\left(h_{\mathrm{mas,w}}-h_{\mathrm{ma}}\right)+\left(1-\mathrm{Le_f}\right)\left(\omega_{\mathrm{s,w}}-\omega\right)h_{\mathrm{v}}\right] \tag{4}$$

where $h_{\mathrm{mas,w}}$ and h_{v} are the saturated moist air specific enthalpy at water temperature and water vapor specific enthalpy, respectively. The $\mathrm{Le_f}$ is a non-dimensional value representing the relative rate of heat transfer and mass transfer between the gas-liquid two-phase, which can be calculated by using the empirical formula given by Bosnjakovic [21]:

$$\mathrm{Le_f}=0.865^{2/3}\left(\frac{\omega_{\mathrm{s,w}}+0.622}{\omega+0.622}-1\right)/\ln\left(\frac{\omega_{\mathrm{s,w}}+0.622}{\omega+0.622}\right) \tag{5}$$

The change rate of seawater salinity, S, along the z-axis can be presented [14, 22]:

$$\frac{\mathrm{d}S}{\mathrm{d}z}=-S\frac{\dot{m}_{\mathrm{a}}}{\dot{m}_{\mathrm{sw}}}\frac{\mathrm{d}\omega}{\mathrm{d}z}=\frac{-SK_{D}A}{\dot{m}_{\mathrm{sw}}}\left(\omega_{\mathrm{s,w}}-\omega\right) \tag{6}$$

When the h_{ma} and ω are determined, the air dry-bulb temperature, T_{a}, and air wet-bulb temperature, T_{wb}, at any control volume along the tower height can be calculated [6]:

$$h_{\mathrm{ma}}=c_{p,\mathrm{a}}\left(T_{\mathrm{a}}-273.15\right)+\omega\left[h_{\mathrm{fgwo}}+c_{p,\mathrm{v}}\left(T_{\mathrm{a}}-273.15\right)\right]=c_{p,\mathrm{ma}}\left(T_{\mathrm{a}}-273.15\right)+\omega h_{\mathrm{fgwo}} \tag{7}$$

$$\omega=\left[\frac{2501.6-2.3263\left(T_{\mathrm{wb}}-273.15\right)}{2501.6+1.8577\left(T-273.15\right)-4.184\left(T_{\mathrm{wb}}-273.15\right)}\right]\left(\frac{0.62509p_{\mathrm{vwb}}}{p_{\mathrm{a}}-1.005p_{\mathrm{vwb}}}\right)-$$
$$-\left[\frac{1.00416\left(T-T_{\mathrm{wb}}\right)}{2501.6+1.8577\left(T-273.15\right)-4.184\left(T_{\mathrm{wb}}-273.15\right)}\right] \tag{8}$$

The calculation equations of seawater and air thermophysical properties involved in eqs. (1)-(8) can be obtained from the literature [6, 14].

To solve the aforementioned governing equations, the following boundary conditions are required:

- At the top of the cooling tower ($z=0$): seawater inlet temperature, $T_{\mathrm{sw,in}}$, seawater inlet mass-flow rate, $\dot{m}_{\mathrm{sw,in}}$, seawater inlet salinity, S_{in}.
- At the bottom of the cooling tower ($z=H$): air inlet dry-bulb temperature, $T_{\mathrm{a,in}}$, air inlet wet-bulb temperature, $T_{\mathrm{wb,in}}$, air inlet mass-flow rate, $\dot{m}_{\mathrm{a}}$, air inlet humidity ratio, ω_{in}.

The tower characteristics equation

The number of cooling tasks based on the freshwater tower can be represented as shown in eq. (9). The integral can be solved via the Simpson method, when the water temperature difference between the tower inlet and outlet, ΔT_{sw}, is less than 15 °C, it has attained sufficient accuracy [23]:

$$N=\frac{KK_{\mathrm{D}}AH}{\dot{m}_{\mathrm{sw,in}}}=\int_{T_{\mathrm{sw,out}}}^{T_{\mathrm{sw,in}}}\frac{c_{p,\mathrm{sw}}}{h_{\mathrm{as}}-h_{\mathrm{a}}}\mathrm{d}T_{\mathrm{sw}}=\frac{c_{p,\mathrm{sw}}\Delta T_{\mathrm{sw}}}{6}\left(\frac{1}{h_{\mathrm{as,wo}}-h_{\mathrm{a,in}}}+\frac{4}{h_{\mathrm{as,wm}}-h_{\mathrm{a,m}}}+\frac{1}{h_{\mathrm{as,wi}}-h_{\mathrm{a,out}}}\right) \tag{9}$$

where

$$K=1-\frac{T_{\mathrm{sw,out}}}{586-0.56\left(T_{\mathrm{sw,out}}-20\right)}$$

is the evaporation correction factor. The $h_{as,wi}$, $h_{as,wo}$, and $h_{as,wm}$ represent the saturated air enthalpy of the inlet water temperature, the saturated air enthalpy of the outlet water temperature, and the saturated air enthalpy of the average water temperature, respectively. The $h_{a,in}$, $h_{a,out}$, and $h_{a,m}$ represent the inlet air enthalpy, the outlet air enthalpy, and the average enthalpy of both, respectively.

The number of cooling characteristics can be obtained from the freshwater tower experimental packing data [24]:

$$N' = Kx\lambda^{y} \tag{10}$$

where λ is the air to water mass-flow ratio, and x and y are empirical constants. For the seawater cooling tower, eq. (10) needs to be multiplied by the corrected coefficient x_s, with the [25], indicating the influence of salt content on the thermal performance of the cooling tower. The modified formula:

$$N' = Kx_s x\lambda^{y} \tag{11}$$

$$\lambda = \frac{\dot{m}_a}{\dot{m}_{sw}} = \frac{\rho_a GA}{\rho_{sw}\dfrac{LA}{3600}} \tag{12}$$

$$x_s = 1 - 1.97\cdot 10^{-3} S_{in} \tag{13}$$

The calculation formula of the volumetric mass transfer coefficient, K_D, of the seawater cooling tower packing zone can be obtained via eqs. (9) and (11):

$$K_D = x_s x\left(\frac{\dot{m}_{sw,in}}{AH}\right)\lambda^{y} \tag{14}$$

Exergy calculation

Exergy analysis is a useful method to complement energy analysis. Exergy analysis can effectively identify any irreversible loss in the tower, and then direct subsequent system improvements. Seawater and moist air are the steady flow working substances within the cooling tower, of which the exergy can be divided into physical and chemical exergy. For steady flow working substances, the kinetic energy and potential energy are often neglected, thus the physical exergy is also called the enthalpy exergy and is composed of thermomechanical exergy and mechanical exergy. The enthalpy exergy represents the maximum useful work that the working substance can do when it changes state through a reversible process to being at thermal and pressure equilibrium with the environmental state. Its characteristic is that the working substance composition does not change, and the equilibrium state at this time is known as the restricted dead state. Chemical exergy is the maximum useful work that the working substance can do when it reaches the dead state through the reversible process from the restricted dead state, and its characteristic is that the composition of the working substance changes [26, 27].

The working substance exergy is the relative value calculated based on the selected dead state (environmental condition). The exergy of the working substance under the dead state is 0. The dead state conditions used for exergy analysis in this paper are the average state of the local outdoor environment during the summer; $t_0 = 27$ °C, $p_0 = 101325$ Pa, and $\omega_0 = 0.0174$ kg$_w$/kg$_a$ (RH$_0$ = 77%, $t_{wb,0} = 23.84$ °C).

Moist air can be considered as an ideal gas composed of dry air and water vapor. The exergy of moist air can be expressed as [28]:

$$E_{\mathrm{ma}}=\dot{m}_a\left\{\left(c_{p,\mathrm{a}}+\omega c_{p,\mathrm{v}}\right)\left(T-T_0-T_0\ln\frac{T}{T_0}\right)+\left(1+1.608\omega\right)\mathrm{R}_\mathrm{a}T_0\ln\frac{p}{p_0}+\right.$$
$$\left.+\mathrm{R}_\mathrm{a}T_0\left[\left(1+1.608\omega\right)\ln\frac{1+1.608\omega_0}{1+1.608\omega}+1.608\omega\ln\frac{\omega}{\omega_0}\right]\right\} \tag{15}$$

where the first term in the bracket on the right-hand side denotes the thermomechanical exergy, the second term in the bracket denotes the mechanical exergy, and the third term in the bracket is the chemical exergy. Since the pressure of moist air is equal to the ambient pressure and assuming that the pressure in the cooling tower does not change ($p = p_0$), the eq. (15) can be modified:

$$E_{\mathrm{ma}}=\dot{m}_\mathrm{a}\left\{\left(c_{p,\mathrm{a}}+\omega c_{p,\mathrm{v}}\right)\left(T-T_0-T_0\ln\frac{T}{T_0}\right)+\right.$$
$$\left.+\mathrm{R}_\mathrm{a}\,T_0\left[\left(1+1.608\omega\right)\ln\frac{1+1.608\omega_0}{1+1.608\omega}+1.608\omega\ln\frac{\omega}{\omega_0}\right]\right\} \tag{16}$$

The heat and mass transfer process in the cooling tower is directly related to the phase change process of water. Ignoring the compressibility of water, the exergy of seawater can be represented [29]:

$$E_{\mathrm{sw}}=\dot{m}_{\mathrm{sw}}\left[c_{p,\mathrm{sw}}\left(T_{\mathrm{sw}}-T_0-T_0\ln\frac{T_{\mathrm{sw}}}{T_0}\right)+v_{\mathrm{sw}}\left(p_{\mathrm{sw}}-p_{\mathrm{sw},0}\right)-\mathrm{R}_\mathrm{v}T_0\ln\left(\mathrm{RH}_0\right)\right] \tag{17}$$

where the first term in the bracket on the right-hand side denotes the thermomechanical exergy, the second term in the bracket denotes the mechanical exergy, and the third term in the bracket is the chemical exergy. The mechanical exergy can be ignored, so the eq. (17) can be modified:

$$E_{\mathrm{sw}}=\dot{m}_{\mathrm{sw}}\left[c_{p,\mathrm{sw}}\left(T_{\mathrm{sw}}-T_0-T_0\ln\frac{T_{\mathrm{sw}}}{T_0}\right)\mathrm{R}_\mathrm{v}T_0\ln\left(\mathrm{RH}_0\right)\right] \tag{18}$$

Cooling tower performance evaluation index

Cooling efficiency

The cooling efficiency describes the ratio of the real cooling capacity of the cooling tower to the theoretical maximum cooling capacity. The greater the cooling efficiency, the closer the cooling tower outlet water temperature to the theoretical limit cooling temperature (inlet air wet-bulb temperature) [30]:

$$\eta_\mathrm{c}=\frac{T_{\mathrm{sw,in}}-T_{\mathrm{sw,out}}}{T_{\mathrm{sw,in}}-T_{\mathrm{wb,in}}} \tag{19}$$

Thermal efficiency

The thermal efficiency can be described as the ratio of the real heat transfer (enthalpy change in the air-side) to the maximum heat transfer (maximum enthalpy change). The maximum heat transfer may occur when the outlet air is saturated and the air temperature is equal to the inlet water temperature [31]:

$$\eta_{\mathrm{T}} = \frac{h_{\mathrm{ma,out}} - h_{\mathrm{ma,in}}}{h_{\mathrm{mas,w}} - h_{\mathrm{ma,in}}} \tag{20}$$

Exergy efficiency

The cooling tower is effectively an evaporative heat exchanger. Its main function is to transfer the energy of the thermal fluid (seawater) to the cold fluid (moist air), and the effective energy (exergy) is the portion that can be used or transferred. Therefore, the exergy efficiency (second-low efficiency) reflects the degree of exergy transfer. The exergy efficiency of the cooling tower can be expressed as the ratio of air exergy change to seawater exergy change [32]:

$$\eta_{\mathrm{E}} = \frac{E_{\mathrm{ma,out}} - E_{\mathrm{ma,in}}}{E_{\mathrm{sw,in}} - E_{\mathrm{sw,out}}} \tag{21}$$

Solution and verification of the mathematical model

Solution methodology

The mathematical model solution process was developed independently using C language in the programming software. The mathematical model was discretized into algebraic equations by the finite difference method and then solved by iterative principle. To facilitate iterative calculation, it was necessary to normalize the two-sided boundary conditions at the top (z = 0) and bottom (z = H) of the tower to the single-sided boundary conditions at the bottom (z = H) of the tower. The solution starts from the bottom (z = H) of the tower (*i.e.*, at the air inlet and water outlet) to the top along the tower height direction and the value of the next iteration step (k + 1) can be calculated from the known value of the current iteration step, k. Since the unknown outlet water conditions at the bottom of the tower taken into account, it is necessary to properly estimate the mass-flow rate, $\dot{m}_{\mathrm{sw,out}}$, temperature, $T_{\mathrm{sw,out}}$, and salinity, S_{out}, of the seawater so that it can be successfully iteratively calculated until the calculated values matched the actual values. The detailed solution methodology is explained by the flow chart presented in fig. 3.

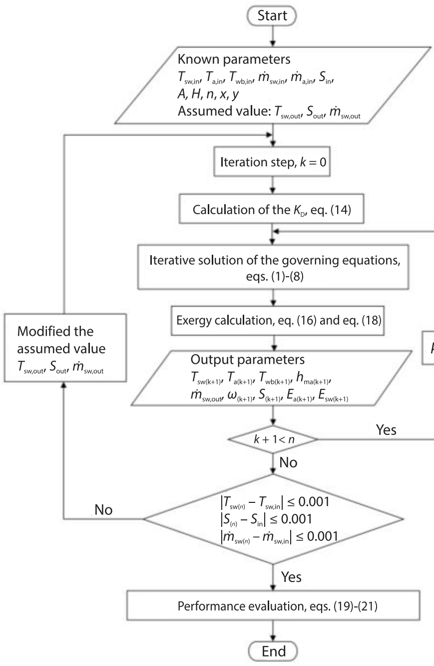

Figure 3. Flow chart of the solution procedure

Mathematical model validation

Considering the calculation accuracy and computation cost, Δz = 0.01 m was selected as the iteration step size. In this paper, the creditability of the calculation model and solution method is determined by relative deviation:

$$\delta = \frac{\left|x_{\text{om}} - x_{\text{oc}}\right|}{x_{\text{om}}} \times 100\% \tag{22}$$

where x_{om} is the experimental value at the outlet and x_{oc} – the calculated value at the outlet.

Table 1 shows the four different operating conditions of the cooling tower experiment in [33]. A comparison was made between the calculation results derived using the proposed mathematical model and the corresponding experimental results obtained from the literature. For each case, the relative deviations for the outlet water temperature, $t_{\text{sw,out}}$, outlet air dry-bulb temperature, $t_{\text{a,out}}$, outlet air humidity ratio, ω_{out}, outlet water exergy, $E_{\text{sw,out}}$, and outlet air exergy, $E_{\text{a,out}}$, between the predicted values and the corresponding experimental results are given in tab. 2. As observed, the calculated values are in good agreement with the literature experimental values. The maximum relative deviations of $t_{\text{sw,out}}$, $t_{\text{a,out}}$, ω_{out}, $E_{\text{sw,out}}$, and $E_{\text{a,out}}$ are 4.62%, 1.36%, 4.00%, 3.99%, and 14.16%, respectively. Therefore, it can be considered that the calculation model and solution method in this paper are reliable.

Table 1. The operating conditions of the cooling tower experiment in the literature

S [gkg^{-1}]	Packing specifications [m]	K_{D} [kgm^{-3}s^{-1}]	$\dot{m}_{\text{sw,in}}$ [kgs^{-1}]	$\dot{m}_{\text{a,in}}$ [kgs^{-1}]	$t_{\text{a,in}}$ [°C]	$t_{\text{wb,in}}$ [°C]	$t_{\text{sw,in}}$ [°C]
0	0.3 × 0.3 × 0.6	0.40	0.065	0.074	30.00	25.00	52.00
0	0.3 × 0.3 × 0.6	0.31	0.056	0.069	30.00	23.00	56.00
0	0.3 × 0.3 × 0.6	0.72	0.065	0.053	26.00	23.00	38.20
0	0.3 × 0.3 × 0.6	0.29	0.056	0.033	30.00	21.00	42.50

Table 2. Comparison of literature experimental results and numerical calculation results

Experimental value					Calculated value					Relative deviation				
$t_{\text{sw,out}}$ [°C]	$t_{\text{a,out}}$ [°C]	ω_{out} [kg$_{\text{w}}$kg$_{\text{a}}^{-1}$]	$E_{\text{sw,out}}$ [kW]	$E_{\text{a,out}}$ [kW]	$t_{\text{sw,out}}$ [°C]	$t_{\text{a,out}}$ [°C]	ω_{out} [kg$_{\text{w}}$kg$_{\text{a}}^{-1}$]	$E_{\text{sw,out}}$ [kW]	$E_{\text{a,out}}$ [kW]	$\delta t_{\text{sw,out}}$ [%]	$\delta t_{\text{a,out}}$ [%]	$\delta\omega_{\text{out}}$ [%]	$\delta E_{\text{sw,out}}$ [%]	$\delta E_{\text{a,out}}$ [%]
40.00	34.73	0.031	6.221	0.224	41.822	34.331	0.03178	6.218	0.204	4.56	1.15	2.52	0.05	8.93
42.00	34.02	0.029	5.287	0.184	43.940	34.481	0.03009	5.367	0.159	4.62	1.36	3.76	1.51	13.59
31.00	30.41	0.027	6.183	0.113	32.060	30.703	0.02751	6.159	0.129	3.42	0.96	1.89	0.39	14.16
36.00	33.36	0.025	4.757	0.069	37.183	33.741	0.02600	4.947	0.074	3.29	1.14	4.00	3.99	7.25

Analysis and discussion

Effect of different salinities

In this paper, four varieties of seawater salinity were selected to analyze the thermal performance of the seawater cooling tower, including S = 0 g/kg (freshwater), S = 35 g/kg (normal seawater), S = 70 g/kg (double concentration), and S = 105 g/kg (three times concentration). The operational and design conditions of the study tower are A = 1.69 m^2, H =1 m, $N = 1.38 \cdot (1 - 1.97 \cdot 10^{-3} S_{\text{in}})\lambda^{0.45}$, L_{in}= 13 m^3/(m^{2}h), G_{in} = 3.2 m/s, $t_{\text{sw,in}}$ = 40 °C, $t_{\text{a,in}}$ = 30 °C, $t_{\text{wb,in}}$= 26 °C. Due to the constant inlet air temperature, the air density remains unchanged and when the inlet air speed is 3.2 m/s, the air mass-flow rate is 6.301 kg/s. Due to different salinities, the density of seawater varies, so the seawater mass-flow rate at the inlet is not consistent when the water-spraying density is maintained at 13 m^3/(m^{2}h). The seawater density, mass-flow rate, outlet temperature, temperature drop, relative humidity, and evaporation loss of the four varieties of salinity previously mentioned is shown in tab. 3.

Table 3. The influence of salinity on important tower parameters

S [gkg^{-1}]	$\dot{m}_{sw,in}$ [kgs^{-1}]	ρ_{sw} [kgm^{-3}]	Evaporation loss [kgs^{-1}]	$t_{sw,out}$ [°C]	Temperature drop [°C]	ω_{out} [g$_w$kg$_a$$^{-1}$]	RH$_{out}$ [%]
0	6.055	992.182	0.088	30.501	9.499	33.643	97.370
35	6.215	1018.321	0.082	30.840	9.160	32.832	95.399
70	6.374	1044.460	0.077	31.209	8.791	32.003	93.303
105	6.534	1070.599	0.072	33.938	6.062	31.167	91.206

As shown in tab. 3, with an increase in salinity, the seawater density increases correspondingly. When the inlet seawater temperature remains constant, the outlet temperature rises with the increased salinity, and the size of the water temperature drop decreases. When the salinity is 105 g/kg, the minimum temperature drop is 6.062 °C, which is 3.437 °C lower than the maximum temperature drop (S = 0 g/kg). The variation in salinity has a similar influence on the outlet air humidity ratio, relative humidity, and water evaporation loss, which all decrease with increased salinity. This is due to the vapor pressure of seawater being lower than that of freshwater, which reduces the potential for water evaporation. The evaporation loss is approximately 6.8-18.2% lower than that of freshwater. The air at the outlet is almost saturated, and the maximum relative humidity is about 97.370% for freshwater, when the salinity is 105 g/kg, and the minimum relative humidity is about 91.206% and a decrease of 6.164%.

Effect of inlet air speed

Figure 4 shows the inlet air speed, G_{in}, and tower efficiency (cooling efficiency η_C, thermal efficiency η_T, and exergy efficiency η_E) for different salinity values. This figure is generated from the following set of data: $t_{sw,in}$ = 40 °C, $t_{a,in}$ = 30 °C, $t_{wb,in}$ = 26 °C, L_{in} = 13 m^3/(m^{2}h), and the G_{in} varies from 3.1-3.6 m/s at an interval of 0.1 m/s.

As shown in fig. 4(a), the η_C increases linearly with the increase in G_{in}. This is due to increased air speed resulting in a decrease in outlet water temperature, so the cooling range (temperature drop, $t_{sw,in} - t_{sw,out}$) increases, and the temperature difference between the inlet water temperature and the inlet air wet-bulb temperature ($t_{sw,in} - t_{wb,in}$) remains constant. These factors together lead to an increase in η_C. The maximum η_C is obtained at S = 0 g/kg and G_{in} = 3.6 m/s, which is about 70.64%, a change of roughly 3.56%, for the measured G range. With the increase in salinity, the η_C is reduced to roughly 2.40-8.25% lower than that of freshwater.

The increased air speed leads to the shortening of the contact time between the seawater and the air, which is embodied in the decrease in the outlet air enthalpy and resulting in the decrease of η_T. As shown in fig. 4(b), when S = 0 g/kg and G_{in} = 3.1 m/s, the maximum η_T is about 48.29%. With an increase of 0.5 m/s in air speed (G_{in} = 3.6 m/s), the η_T decreases to 43.86%, a decrease of 4.43%. With increased salinity, the η_T is reduced to about 1.06-3.09% lower than that of freshwater, indicating that changes in salinity have more effect on the η_C than the η_T, under the same working conditions.

Figure 4(c) shows the change in η_E. It can be seen that η_E decreases with increasing G_{in}, due to the outlet water exergy decrease, whilst the inlet water exergy and the exergy difference between the inlet and outlet air ($E_{ma,out} - E_{ma,in}$) stays constant. When G_{in} = 3.1 m/s and S = 0 g/kg, the maximum η_E is approximately 56%, indicating that roughly 56% of the energy can be effectively utilized and converted in the heat and mass transfer process between seawater and air. In other words, about 44% of the energy is dissipated due to the irreversible exergy loss during the heat and mass transfer process. When G_{in} is 3.6 m/s and the salinity is 0 g/kg, the η_E is 54.10% and a 1.9% reduction. However, when the salinity increases to 35 g/kg, the η_E decreases to 51.63% which affects the exergy performance of the cooling tower. Therefore, to provide the same efficiency under the new conditions, the G_{in} needs to be decreased to about 3 m/s. The η_E decreases with a salinity range between 0 g/kg and 105 g/kg, which is about 2.47-7.73% lower than freshwater.

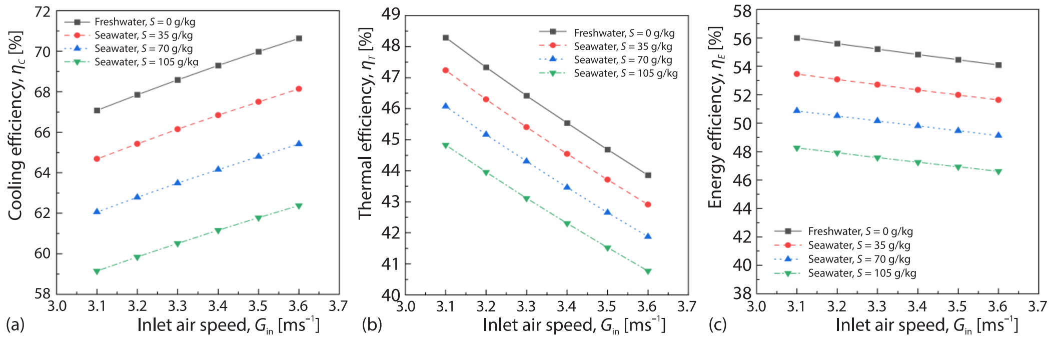

Figure 4. The influence of inlet air speed onwer efficiency under different salinity; (a) cooling efficiency, η_c, (b) thermal efficiency, η_T, and (c) exergy efficiency, η_E

Effect of inlet air wet-bulb temperature

Figure 5 is the plot between the inlet air wet-bulb temperature, $t_{wb,in}$, and tower efficiency (cooling efficiency η_C, thermal efficiency η_T, and exergy efficiency η_E) for different values of salinity. This figure is generated from the following set of data: $t_{sw,in}$ = 40 °C, $t_{a,in}$ = 30 °C, L_{in} = 13 m^3/(m^{2}h), G_{in} = 3.2 m/s, and $t_{wb,in}$ is selected from 25-27 °C at intervals of 0.5 °C, due to the limitations of the inlet air dry-bulb temperature, and the reference environmental conditions in the exergy calculation.

Compared with the inlet air speed, the changes in the air inlet wet-bulb temperature have little effect on the η_C, but it does still slightly increase with increasing $t_{wb,in}$, as shown in fig. 5(a). When the $t_{wb,in}$ rose from 25-27 °C, the η_C increased by about 2.01%, 1.72%, 1.43%, and 1.13% for salinities of 0 g/kg, 35 g/kg, 70 g/kg, and 105 g/kg, respectively. The maximum η_C was about 68.86% at S = 0 g/kg and $t_{wb,in}$ = 27 °C. With the increase in salinity, the η_C was about 2.28-8.47% lower than freshwater.

As shown in fig. 5(b), when the salinity increases from 0 g/kg to 105 g/kg, the η_T reduces noticeably, and is about 1.03-3.37% lower than that of freshwater. However, when the salinity remains unchanged, as the $t_{wb,in}$ rises from 25-27 °C, there is no appreciable change in η_T. The η_T remains about 47.33%, 46.30%, 45.17%, and 43.96% for salinities of 0 g/kg, 35 g/kg, 70 g/kg, and 105 g/kg, respectively.

Figure 5(c) shows that when $t_{wb,in}$ increases from 25-27 °C, the η_E increases noticeably. This is because the outlet seawater exergy ($t_{sw,out}$ increases with increasing $t_{wb,in}$), and the inlet and outlet air exergy (air temperature and humidity ratio increase with increasing $t_{wb,in}$) are all affected by the $t_{wb,in}$. Changes in $t_{wb,in}$ have more effect on η_E compared to changes in G_{in}, with the minimum η_E about 50.39% at S = 0 g/kg and $t_{wb,in}$ = 25 °C. With an increase of 2 °C in the $t_{wb,in}$ (27 °C), the maximum η_E is about 60.41%, an increase of approximately 10.02%. When the $t_{wb,in}$ is 25 °C and the salinity is 35 g/kg, the η_E is 47.76%. However, when the salinity increases to 70 g/kg, the η_E decreases to 45.09%. This affects the exergy performance of the cooling tower. Therefore, to provide the same efficiency under the new conditions, the $t_{wb,in}$ needs to be increased by about 0.5 °C. With the increase in salinity, the η_E is about 2.44-7.99% lower than that of freshwater.

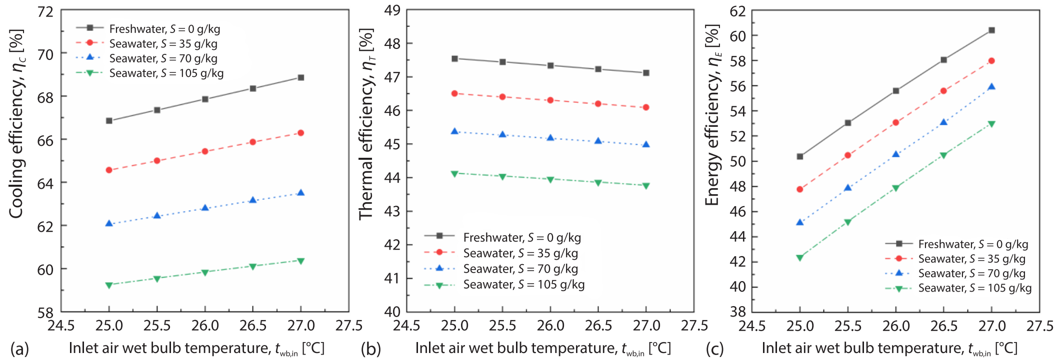

Figure 5. The influence of inlet air wet-bulb temperature onwer efficiency with different salinities; (a) cooling efficiency, η_c, (b) thermal efficiency, η_T, and (c) exergy efficiency, η_E

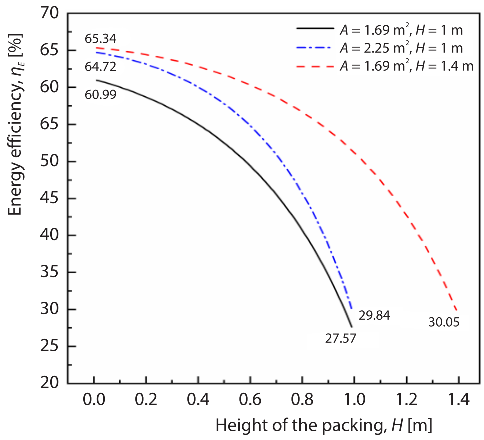

Figure 6. Exergy efficiency along the tower for different packing types

Tower performance improvement based on exergy analysis

The reference operating conditions are: A = 1.69 m^2, H = 1 m, L_{in} = 13 m^3/(m^{2}h), G_{in} = 3.2 m/s, $t_{sw,in}$ = 40 °C, $t_{a,in}$ = 30 °C, $t_{wb,in}$ = 26 °C, and S_{in} = 35 g/kg. Furthermore, exergy analysis can be used as a guideline to identify opportunities to improve the performance of seawater cooling towers. The distribution of the exergy efficiency in the tower is plotted in fig. 6. It can be seen that the exergy efficiency distribution is high at the top (z = 0 m) and gradually reduces at the bottom of the packing (z = 1 m). Hence, the potential for improvement is higher at the bottom of the packing zone. When the packing cross-sectional area, A, increases from 1.69-2.25 m^2, the exergy efficiency at the bottom increases to 29.84%, a rise of about 2.27%. Under the conditions of A = 2.25 m^2 and H = 1 m, the exergy efficiency distribution in the tower improves compared to the reference condition. The cooling, thermal, and exergy efficiency of the whole tower are increased by 6.76%, 4.86%, and 5.13%, respectively, as shown in tab. 4. When the packing height, H, increases from 1-1.4 m, there is a significant improvement in exergy efficiency distribution compared to the reference condition. The exergy efficiency at the bottom increases to 30.05%, an increase of approximately 2.48%. The cooling, thermal, and exergy efficiency of the whole tower are increased by 7.91%, 5.44%, and 6.03%, respectively.

The exergy analysis results, apart from the changes in packing specification, demonstrate that it can improve the cooling tower's performance, and a change in the cooling tower's operating conditions can also achieve the same result. The response surface in fig. 7 shows that the exergy efficiency increases with increasing air wet-bulb temperature and decreasing air speed. It can be seen from the contour plot in fig. 7 that the maximum exergy efficiency (62.40 %) is achieved at G_{in} = 1.7 m/s and $t_{wb,in}$ = 27 °C. Compared with the reference conditions, the thermal efficiency and exergy efficiency of the whole tower are increased by 19.19% and 9.33%, respectively. However, the cooling efficiency decreased by 15.11%. Therefore, we need to comprehensively consider the weight of every evaluation index to systematically improve the heat and mass transfer performance and exergy performance of seawater cooling towers.

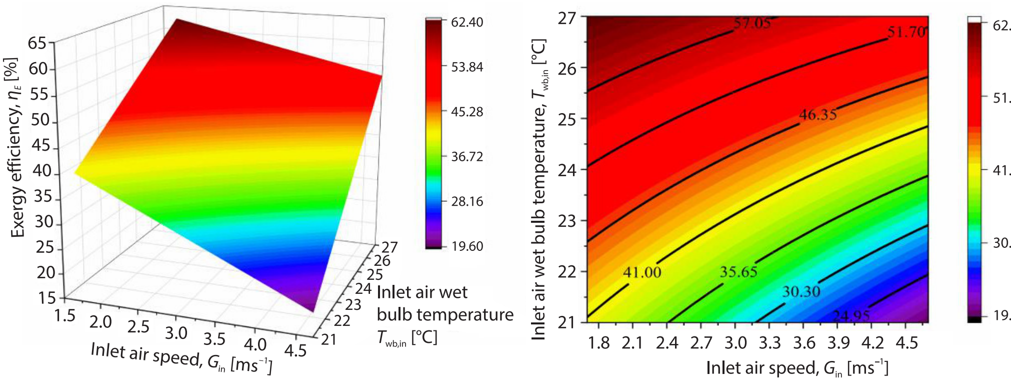

Figure 7. The 3-D surface and contour maps showing the effect of operating conditions on exergy efficiency

Table 4. Exergy analysis results

	η_C [%]	η_T [%]	η_E [%]
Reference conditions	65.43	46.30	53.07
A = 2.25 m^2, H = 1 m	72.19	51.16	58.20
A = 1.69 m^2, H = 1.4 m	73.34	51.74	59.10
G_{in} = 1.7 m/s, $t_{wb,in}$ = 27 °C	50.32	65.49	62.40

Conclusions

In this research, a detailed mathematical model for evaluating the heat and mass transfer performance and exergy performance of MDCWSCT was established. The numerical solution was implemented based on the computer program developed by the VC^{++} framework. Furthermore, the calculation model and solution method were validated by the experimental results reported by the literature. The calculated results correspond highly with the experimental results. The influence of salinity, air speed, and air wet-bulb temperature on cooling efficiency, thermal efficiency, and exergy efficiency were analyzed. The conclusions of this study are as follows.

- Increases in salinity have a significant effect on the water density and outlet water temperature under the study conditions. With increases in salinity, the evaporation of water, air humidity ratio, and relative humidity are lower than that of freshwater, due to the decrease in vapor pressure.
- When the air speed varies from 3.1-3.6 m/s and all other conditions remain unchanged, the η_C increases by 3.46%, the η_T decreases by 4.32 %, and the η_E decreases by 1.82% for normal salt content seawater (35 g/kg). With increases in salinity, the η_C, η_T, and η_E are approximately 2.40-8.25%, 1.06-3.09%, and 2.47-7.73% lower than that of freshwater, respectively.
- When the air wet-bulb temperature varies from 25-27 °C and all other conditions remain unchanged, the η_C increases by 1.72% and the η_E increases by 10.21% for normal salt content seawater (35 g/kg). There is no appreciable change in η_T, and it remains around 47.33%, 46.30%, 45.17%, and 43.96% for salinities of 0 g/kg, 35 g/kg, 70 g/kg, and 105 g/kg, respec-

tively. With increases in salinity, the η_C, η_T, and η_E are around 2.28-8.47%, 1.03-3.37%, and 2.44-7.99% lower than that of freshwater, respectively.

- Compared to air wet-bulb temperature, changes in air speed have more influence on η_C and η_T under the study conditions. Moreover, the air wet-bulb temperature is the most significant parameter affecting η_E. The influence of seawater salinity on η_C and η_E is greater than on η_T under the same conditions.
- The seawater cooling tower exergy analysis, demonstrates that the heat and mass transfer performance and exergy performance can be improved by selecting the optimum operating conditions and appropriate packing specifications.

Acknowledgment

This paper is supported by National Natural Science Foundation of China (No. 51879154 & 51806128), Shandong Provincial Natural Science Foundation of China (No. ZR-2019MEE007) and SDUT & Zhangdian District Integration Development Project (118239). These supports are gratefully acknowledged.

Nomenclature

A – cross-sectional area of packing, [m^2]
c_p – specific heat at constant pressure, [kJkg^{-1}K^{-1}]
E – exergy, [kW]
G – air speed, [ms^{-1}]
H – height of tower (packing), [m]
h – specific enthalpy, [kJkg^{-1}]
h_{fgwo} – latent heat of vaporization at 0 °C
K_D – volumetric mass transfer coefficient, [kgm^{-3}s^{-1}]
L – water-spraying density, [m^{3}m^{-2}h^{-1}]
$\mathrm{Le_f}$ – Lewis factor
$\dot{m}$ – mass-flow rate, [kgs^{-1}]
p – pressure, [Pa]
Q – heat dissipation, [kW]
RH – relative humidity, [%]
$\mathrm{R_a}$ – gas c onstant of dry air, 0.287, [kJkg^{-1}K^{-1}]
$\mathrm{R_v}$ – gas constant of vapor, 0.461, [kJkg^{-1}K^{-1}]
S – salinity, [gkg^{-1}]
T, t – temperature, [K] [°C]
z – vertical co-ordinate [m]

Greek symbols

δ – relative deviation, [%]
η – efficiency, [%]
λ – air to water mass-flow ratio
ρ – density, [kgm^{-3}]
ω – humidity ratio of moist air, [kg$_w$kg$_a$$^{-1}$]

Subscripts

0 – dead state (environmental condition)
a – air/dry-bulb
in – inlet of the tower
ma – moist air
out – outlet of the tower
sw – saturated moist air at the seawater temperature
s,w – seawater
v – vapor dry
wb – wet-bulb

References

[1] Nester, D. M., Salt Water Cooling Tower, *Chemical Engineering Progress*, *67* (1971), 7, pp. 49-51
[2] Fu, Q., *et al*., Seawater Cycling Cooling and Its Industrial Application, *Proceedings*, 3rd International Conference on Material, Mechanical and Manufacturing Engineering, Guangzhou, China, 2015, Vol. 3, pp. 1758-1762
[3] Yan, M., *et al*., Comparative Study on the Cooling Performance of Evaporative Cooling Systems Using Seawater and Freshwater, *International Journal of Refrigeration*, *121* (2021), 10, pp. 23-32
[4] Al-Bloushi, M., *et al*., Performance Assessment of Oxidants as a Biocide for Biofouling Control in Industrial Seawater Cooling Towers, *Journal of Industrial and Engineering Chemistry*, *59* (2018), 10, pp. 127-133
[5] Guo, Q. J., *et al*., An Analytical Approach to Wet Cooling Towers Based on Functional Analysis, *Mathematical Problems in Engineering*, *2019* (2019), 12, pp. 1-9
[6] Kloppers, J. C., Kroger, D. G., A Critical Investigation into the Heat and Mass Transfer Analysis of Counterflow Wet-Cooling Towers, *International Journal of Heat and Mass Transfer*, *48* (2005), 3-4, pp. 765-777

[7] Zengin, G., Onat, A., Experimental and Theoretical Analysis of Mechanical Draft Counterflow Wet Cooling Towers, *Science and Technology for the Built Environment*, *27* (2020), 1, pp. 14-27
[8] Llano-Restrepo, M., Monsalve-Reyes, R., Modelling and Simulation of Counterflow Wet-Cooling Towers and the Accurate Calculation and Correlation of Mass Transfer Coefficients for Thermal Performance Prediction, *International Journal of Refrigeration*, *74* (2017),10, pp. 47-72
[9] Khan, J. U. R., *et al*., Performance Characteristics of Counter Flow Wet Cooling Towers, *Energy Conversion and Management*, *44* (2003), 13, pp. 2073-2091
[10] Papaefthimiou,V. D., *et al*., Thermodynamic Study of Wet Cooling Tower Performance, *International Journal of Energy Research*, *30* (2006), 6, pp. 411-426
[11] Muangnoi, T., Effects of Inlet Relative Humidity and Inlet Temperature on the Performance of Counterflow Wet Cooling Tower Based on Exergy Analysis, *Energy Conversion and Management*, *49* (2008), 10, pp. 2795-2800
[12] Muangnoi, T., *et al*., An Exergy Analysis on the Performance of a Counterflow Wet Cooling Tower, *Applied Thermal Engineering*, *27* (2007), 5-6, pp. 910-917
[13] Qureshi, B. A., Zubair, S. M., Second-Law-Based Performance Evaluation of Cooling Towers and Evaporative Heat Exchangers, *International Journal of Thermal Sciences*, *46* (2007), 2, pp. 188-198
[14] Sharqawy, M. H., *et al.*, On Thermal Performance of Seawater Cooling Towers, *Journal of Engineering for Gas Turbines and Power-Transactions of the Asme*, *133* (2011), 4, pp. 1-7
[15] Sharqawy, M. H., *et a*l., Thermal Performance Evaluation of Seawatr Cooling Towers, *Proceedings*, ASME International Mechanical Engineering Congress and Exposition (IMECE), Denver, Co., USA, 2011, Vol. 1, pp. 1-7
[16] Qi, X. N., *et al*., Performance Prediction of Seawater Shower Cooling Towers, *Energy*, *97* (2016), 12, pp. 435-443
[17] Sadafi, M. H., *et al.*, Numerical and Experimental Study on a Single Cone Saline Water Spray in a Wind tunnel, *International Journal of Thermal Sciences*, *120* (2017), 6, pp. 190-202
[18] Wan, D., *et al*., Effect of Cooling Water Salinity on the Cooling Performance of Natural Draft Wet Cooling Tower, *161* (2020), 12, pp. 120-257
[19] Poppe, M., Rogener, H., *Berechnung von Rückkühlwerken* (in German), VDI-Wärmeatlas, Springer, New York, USA, 1991, pp. 1-15
[20] Kroger, D. G., Air-Cooled Heat Exchangers and Cooling Towers, Ph. D. thesis, University of Stellenbosch, Stellenbosch, The Republic of South Africa, 2004
[21] Bosnjakovic, F., *Technische Thermodinamik*, Theodor Steinkopf, Dresden, Germany, 1965
[22] Husain, I., Performance Evaluation of Seawater Counterflow Cooling Tower, Ph. M. thesis, King Fahd University of Petroleum and Minerals, Dhahran, Kingdom of Saudi Arabia, 2011
[23] Khan, J. U. R., Zubair, S. M., An Improved Design and Rating Analyses of Counter Flow Wet Cooling Towers, *Journal of Heat Transfer-Transactions of the Asme*, *123* (2001), 4, pp. 770-778
[24] ***, ASHRAE (American Society of Heating, Refrigerating and Air-Conditioning Engineers), ASHRAE Equipment Guide, ASHRAE, Atlanta, GA, USA, 1983
[25] Wang, F., *et al*., Research on the Characteristics of Water Drenching Fillers of Seawater Cooling Tower in Nuclear Power Station (in Chinese), *Water & Wastewater*, *52* (2016), 2, pp. 60-64
[26] Dovjak, M., *et al*., Exergy Analysis of Conventional and Low Exergy Systems for Heating and Cooling of Near Zero Energy Buildings, *Journal of Mechanical Engineering*, *58* (2012), 7-8, pp. 453-461
[27] Qi, X. N., *et al*., Exergy Based Performance Analysis of a Shower Cooling Tower, *Strojniski Vestnik-Journal of Mechanical Engineering*, *59* (2013), 4, pp. 251-259
[28] Bejan, A., *Advanced Engineering Thermodynamics*, Wiley & Sons, Inc., Singapore, 1997
[29] Wark, K., *Advanced Thermodynamics for Engineers*, Elsevier., New York, USA, 1995
[30] Cheremisinoff, N. P., *Cheremisinoff, P. N., Cooling Towers*: *Selection, Design, and Practice*, Ann Arbor Science Publishers, Ann Arbor, Mich., USA, 1981
[31] Nellis, G., Klein, S., *Heat Transfer*, Cambridge University Press, Cambridge, UK, 2008
[32] Singh, K., Das, R., Improved Quantification of Exergy Destruction in Mechanical Cooling Tower Considering All Tower Inlet Parameters, *Journal of Heat Transfer*, *140* (2018), 5, pp. 1-14
[33] Akbarpour Ghazani, M., *et a*l., A Comprehensive Analysis of a Laboratory Scale Counter Flow Wet Cooling Tower Using the First and the Second Laws of Thermodynamics, *Applied Thermal Engineering*, *125* (2017), 7, pp. 1389-1401

Paper submitted: May 23, 2021
Paper revised: September 23, 2021
Paper accepted: September 23, 2021